

# Cosmic ray drift, the second knee and galactic anisotropies

Julián Candia<sup>a</sup>, Silvia Mollerach<sup>b</sup> and Esteban Roulet<sup>b</sup>

<sup>a</sup>*Departamento de Física, Universidad Nacional de La Plata, CC67,  
La Plata 1900, Argentina*

<sup>b</sup>*CONICET, Centro Atómico Bariloche, Av. Bustillo 9500,  
Bariloche 8400, Argentina*

October 28, 2018

## Abstract

We show that the second knee in the cosmic ray spectrum (i.e. the steepening occurring at  $E \simeq 4 \times 10^{17}$  eV) could be related to drift effects affecting the heaviest nuclear component, the iron group nuclei, in a scenario in which the knee at  $3 \times 10^{15}$  eV indicates the onset of drift effects in the lighter proton component. We also study the anisotropies resulting from diffusion and drift currents in the Galaxy, showing their potential relevance to account for the AGASA observations at  $E \sim 10^{18}$  eV, before the extragalactic component becomes dominant.

There are a couple of observations regarding cosmic rays (CRs) at energies  $\sim 10^{18}$  eV, i.e. just below the ankle, which still remain puzzling (see e.g. [1, 2]). One is the steepening in the spectrum taking place at an energy  $E_{sk} \simeq 4 \times 10^{17}$  eV, which is most apparent in the Yakutsk [3] and Fly’s Eye stereo [4, 5] data, and is usually referred to as the ‘second knee’, at which the spectral index  $\alpha$  (such that  $dN/dE \propto E^{-\alpha}$ ) changes from  $\alpha \simeq 3$  below  $E_{sk}$  to  $\alpha \simeq 3.3$  above  $E_{sk}$ , although probably in a smooth way. The other is the 4% anisotropy at  $E \simeq 0.8 - 2 \times 10^{18}$  eV reported by the AGASA collaboration [6], with an excess observed from a direction near the galactic center and a (probably associated) deficit near the galactic anticenter direction. Also some excess of events in the direction of the Cygnus region (along the Orion spiral arm) has been observed. An excess from a direction near the galactic center was also found in the SUGAR data [7], but it has a smaller spatial extension (consistent with a point-like source) and its direction is few degrees away from the AGASA reported excess. The fact that these anisotropies are associated to galactic features is quite

important, because it is believed that the galactic cosmic ray component should just be fading away at  $E > 10^{18}$  eV, since the CR spectrum should become dominated by the extragalactic component above the ankle, which lies at energies  $\sim 5 \times 10^{18}$  eV. Hence, the energies at which these features take place are probably the highest ones at which the CR spectrum is still dominated by the galactic component, and the features observed may actually be related with the very same process responsible for the fading away of this component.

In this work we want to show that the steepening of the spectrum at  $E_{sk}$  can be directly related to the enhancement of the escape mechanism of the iron group nuclei due to efficient drift effects, and that the observed anisotropies can be linked to the overall CR motion arising from these drifts. It is interesting that these processes would then be directly related to the scenario in which the knee in the spectrum at  $E_{knee} \simeq 3 \times 10^{15}$  eV results just from the transition from a regime in which the CR transport is dominated by transverse diffusion to one dominated by the Hall diffusion, i.e. by drift effects [8, 9]. This scenario is based on the fact that each CR component of charge  $Z$  starts to be affected by drifts at an energy  $E \simeq Z E_{knee}$ , and its spectrum progressively steepens, with the spectral index finally changing by  $\Delta\alpha \simeq 2/3$  in a decade of energy. The envelope of the total spectrum obtained by adding together the different nuclear components nicely fits the change from a spectrum  $\propto E^{-2.7}$  below the knee, to one  $\propto E^{-3}$  above it. However, above  $10^{17}$  eV, where all the lighter components are strongly suppressed, the dominant iron component will progressively steepen its spectrum until the overall spectrum becomes  $\propto E^{-3.3}$  above a few  $\times 10^{17}$  eV, hence reproducing the behavior observed at the second knee. This scenario also naturally explains the transition towards a heavier composition above the knee reported by several experiments.

The change in the spectrum from the diffusion to the drift dominated regimes can be simply understood from the steady state diffusion equation  $\nabla \cdot \mathbf{J} = Q$ , where  $Q$  is the source and the CR current is related to the CR density  $N$  through

$$\mathbf{J} = -D_{\perp} \nabla_{\perp} N - D_{\parallel} \nabla_{\parallel} N + D_A \mathbf{b} \times \nabla N, \quad (1)$$

with  $\mathbf{b}$  being the unit vector in the direction of the regular magnetic field  $\mathbf{B}_{reg}$ , i.e.  $\mathbf{b} \equiv \mathbf{B}_{reg}/|\mathbf{B}_{reg}|$ , and  $\nabla_{\parallel} = \mathbf{b}(\mathbf{b} \cdot \nabla)$ , while  $\nabla_{\perp} = \nabla - \nabla_{\parallel}$ . The components of the diffusion tensor are  $D_{\parallel}$  (along the direction of  $\mathbf{B}_{reg}$ ),  $D_{\perp}$  in the perpendicular direction, while  $D_A$  is associated to the antisymmetric part and determines the drift effects. Assuming for simplicity that the regular magnetic field is directed in the azimuthal direction and that in a first approach the Galaxy can be considered to have cylindrical symmetry, one finds that  $D_{\parallel}$  plays no role in the diffusion equation. Using now the fact that (for a Kolmogorov spectrum of fluctuations in the turbulent magnetic field component)  $D_{\perp}(\mathbf{x}) \simeq D_{\perp}^0(\mathbf{x})(E/E_0)^{1/3}$ , while  $D_A(\mathbf{x}) \simeq D_A^0(\mathbf{x})E/E_0$  [8], one finds that at low energies ( $E < Z E_{knee}$ ) the transverse diffusion is the dominant process affecting the transport of CRs and leading to  $dN/dE \propto (D_{\perp}^0/D_{\perp})dQ/dE \propto E^{-\beta-1/3}$ ,

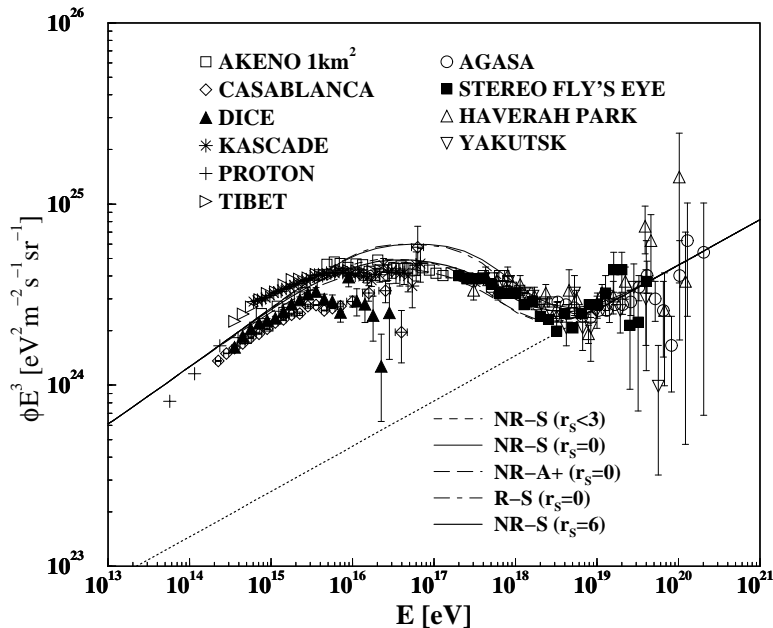


Figure 1: CR spectra computed for different galactic magnetic field models and source locations, which correspond to the same source and model parameters as in Figures 3 and 4 (see more details in the text). The dotted straight line is the extragalactic flux from ref. [1]. Also shown are the relevant experimental data points.

where  $\beta$  is the spectral index of the source, while at high energies ( $E \gg Z E_{knee}$ ) one has instead  $dN/dE \propto (D_A^0/D_A)dQ/dE \propto E^{-\beta-1}$ .

In Figure 1 we display the CR spectrum, computed following ref. [9] for the galactic component, and adding an extragalactic component  $\propto E^{-2.75}$  (with normalization taken from [1]) to fit the observations beyond the ankle. Different curves represent different assumptions for the source distribution and for the galactic magnetic field model. The adopted galactic source spectra are featureless extrapolations of the spectra measured below the knee, and hence the resulting changes in slope are just due to the energy dependence of the diffusion process responsible for the escape of CRs from the Galaxy. The choice of the model parameters was just guided by the requirement of correctly reproducing the first knee, and they are all quite plausible. As is apparent from the figure, the fit to the data is in general remarkably good.

Also notice that if the extragalactic flux can be considered to be isotropic, it will not be enhanced by the Galactic diffusion process if no reacceleration in the Galaxy occurs. This may be understood as being a consequence of the Liouville theorem [10], and can also be seen from the diffusion equations by noting that the solution in the absence of sources and with isotropic boundary conditions at the outskirts of the Galaxy is just to have a constant density, so that there is no way in which an

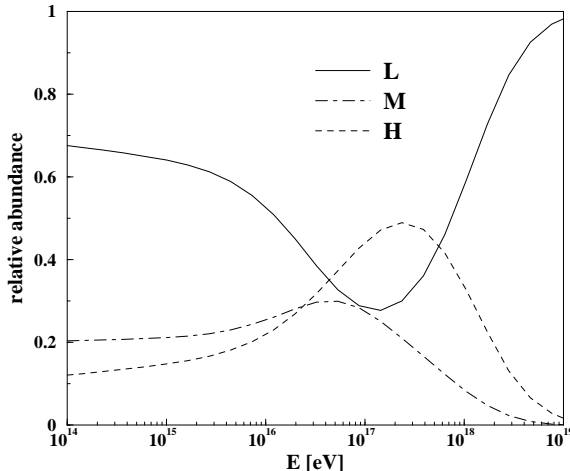


Figure 2: Fractional abundances of different CR components, assuming that the extragalactic flux consists mainly of protons. The elements are grouped into light ( $1 \leq Z \leq 5$ ), medium ( $6 \leq Z \leq 19$ ) and heavy ( $20 \leq Z \leq 26$ ) components. The data correspond to the same source and magnetic field model as in Figure 3.

overdensity in the extragalactic flux could arise from diffusion processes alone.

The relative abundances of different elements vs. energy are plotted in Figure 2, assuming that the extragalactic flux consists mainly of protons. One obtains that in our model the CR composition at  $E \simeq 5 \times 10^{17}$  eV consists of about 50% of galactic iron group nuclei (mostly Fe and Mn), of a proportion ( $\sim 20\%$ ) of intermediate mass galactic nuclei ( $Z = 6-19$ ) while the rest consists essentially of galactic and extragalactic protons. These numbers are quite consistent with the Haverah Park determination of nuclear abundances using the lateral distribution of air showers [11], which suggest that in the range  $2 \times 10^{17}-10^{18}$  eV only  $\sim 30\%$  of the CRs are light, with the rest being mostly heavy nuclear species. Also, the composition change to a lighter mix starting around the energy of the second knee [12] is explained in this scenario as iron group nuclei drift away from the galactic plane with increasing efficiency for increasing energies.

Turning now to consider the anisotropies resulting in this scenario, these will be produced by the galactic cosmic ray component alone, since as just discussed, under the assumption that at  $10^{18}$  eV the extragalactic component is originally isotropic it will remain so after the propagation effects in the Galaxy are taken into account. The anisotropy associated to the galactic component is given by [13]

$$\delta = \frac{3 \mathbf{J}}{c N}, \quad (2)$$

where  $N$  is the total (galactic plus extragalactic) CR density, and  $\mathbf{J}$  is the CR current introduced in Eq. (1).

Under the assumption of cylindrical symmetry and that the regular magnetic field is in the azimuthal direction, one has that  $\nabla_{\perp}N = \nabla N$  and that the CR current will be perpendicular to the regular magnetic field (i.e. lying on the  $r - z$  plane). The contribution to the CR current arising from the transverse diffusion will be in the direction of  $\nabla N$  (and hence orthogonal to the isodensity contours), while the drift part will be orthogonal to  $\nabla N$  (and hence parallel to the isodensity contours). Under these simplifying assumptions, the components of the anisotropy will then read

$$\delta_r = \frac{3}{c N} \left( -D_{\perp} \frac{\partial N}{\partial r} + D_A \text{sign}(B_{reg}^{\phi}) \frac{\partial N}{\partial z} \right), \quad (3)$$

$$\delta_z = \frac{3}{c N} \left( -D_{\perp} \frac{\partial N}{\partial z} - D_A \text{sign}(B_{reg}^{\phi}) \frac{\partial N}{\partial r} \right). \quad (4)$$

In Figures 3 and 4 we display, for different galactic magnetic field and source models, the density contours resulting from the numerical integration of the diffusion equations (solid lines) as well as the direction of the anisotropy vectors and with different shadings the amplitudes of the anisotropies. The results are for given  $E/Z$  values, i.e. for different energies according to which nuclear species are considered. Our location corresponds to  $r_0 = 8.5$  kpc and  $z_0 \simeq 0$ . The relative importance of the diffusion and drift components in the different galactic locations can be directly inferred from the relative directions between the isodensity contours and the arrows. Figure 3.a corresponds to energies well below the first knee ( $E/Z = 10^{14}$  eV), where the diffusion is completely dominated by  $D_{\perp}$ . The source is assumed to be in the galactic plane and to have a constant strength for  $r < 3$  kpc, while vanishing at larger radii. We see that the resulting density contours are symmetric with respect to the galactic plane, and the anisotropies are perpendicular to them and quite small ( $\sim 10^{-4}$ ). Figure 3.b is for an energy corresponding to  $E/Z \simeq E_{knee}$ , where the drift effects start to be non-negligible and the local anisotropies are  $\sim 10^{-3}$ , while figure 3.c corresponds to rigidities such that  $E/Z \simeq 1.5 \times 10^{18}$  eV/26, displaying the behavior that iron nuclei will follow for energies near  $1.5 \times 10^{18}$  eV. In this regime the densities are largely determined by the drifts, and they reflect the general asymmetries of the regular magnetic field at large scales. The local anisotropies are in this case of order  $10^{-2}$ .

Figure 3 was done for a regular magnetic field consisting of a disk component with reversals between arms, a vertical scale height  $z_d = 0.5$  kpc and a local strength  $B_0^{disk} = -0.75 \mu\text{G} \hat{\phi}$ . The halo regular component had no reversals, a scale height  $z_h = 5$  kpc, was symmetric with respect to the galactic plane and had a local value of  $B_0^{halo} = -0.75 \mu\text{G} \hat{\phi}$ . The random component had a similar scale height,  $z_r = 5$  kpc and a local rms value of  $B_0^{rand} = 1.5 \mu\text{G}$  (see ref. [9] for details of the magnetic field profiles adopted). In figure 4 we display results equivalent to those of figure 3.c but for different galactic magnetic field parameters and geometries and for different

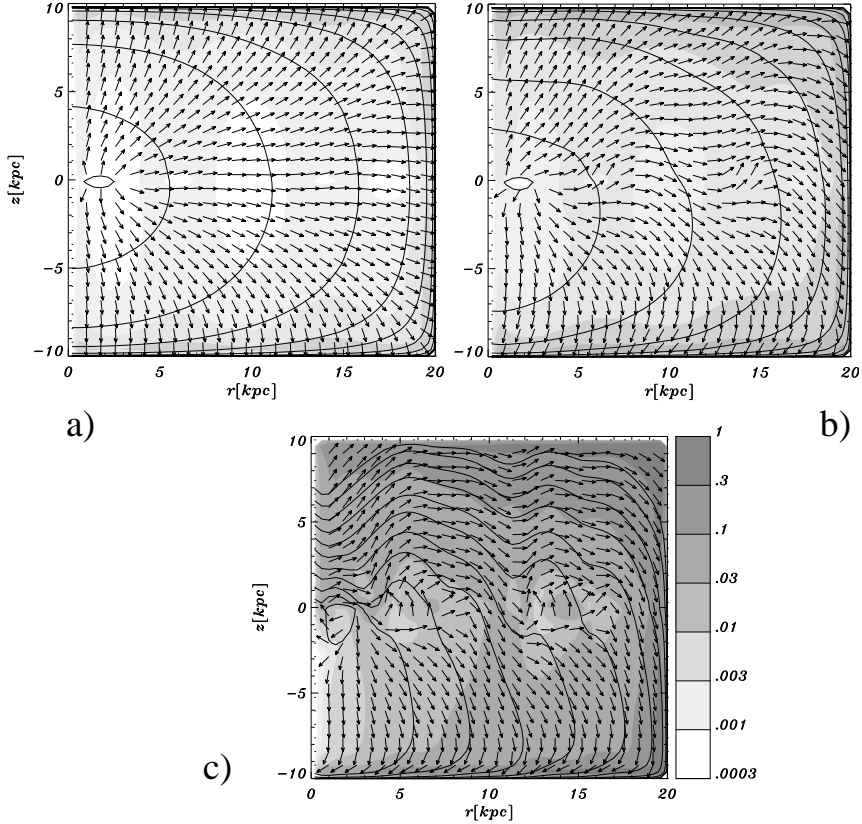


Figure 3: Isodensity contours for different CR energies, with a) corresponding to  $E/Z = 10^{14}$  eV, b) to  $E/Z = E_{knee}$  and c) to  $E/Z = 1.5 \times 10^{18}$  eV/26. Every two contours there is a change by an order of magnitude in the densities. The arrows represent the direction of the anisotropy vectors, while the shadings indicate the amplitude of the anisotropies. The model corresponds to a source in the galactic plane constant inside 3 kpc, and the magnetic field structure described in the text.

source locations  $r_s$ . For instance,  $NR$  corresponds to a halo without reversals, while  $R$  (bottom left panel) corresponds to a halo with reversals similar to those adopted for the disk model. The label  $S(A)$  stands for symmetric (antisymmetric) halo models, i.e. such that  $B_0^{halo}(r, z) = B_0^{halo}(r, -z)$  ( $B_0^{halo}(r, z) = -B_0^{halo}(r, -z)$ ), while the + sign in the  $A+$  label (top right panel) is because  $\text{sign}(B_0^{halo} \cdot B_0^{disk})$  is positive at our galactocentric radius for  $z > 0$ . Clearly the CR densities, the drifts and the corresponding anisotropies vary a lot from model to model, even if all models provide acceptable fits to the local CR spectrum, and hence it is seen that the observed local anisotropies can provide a useful handle to establish the general properties of the galactic magnetic field.

It is important to notice that both the galactic center excess and the galactic

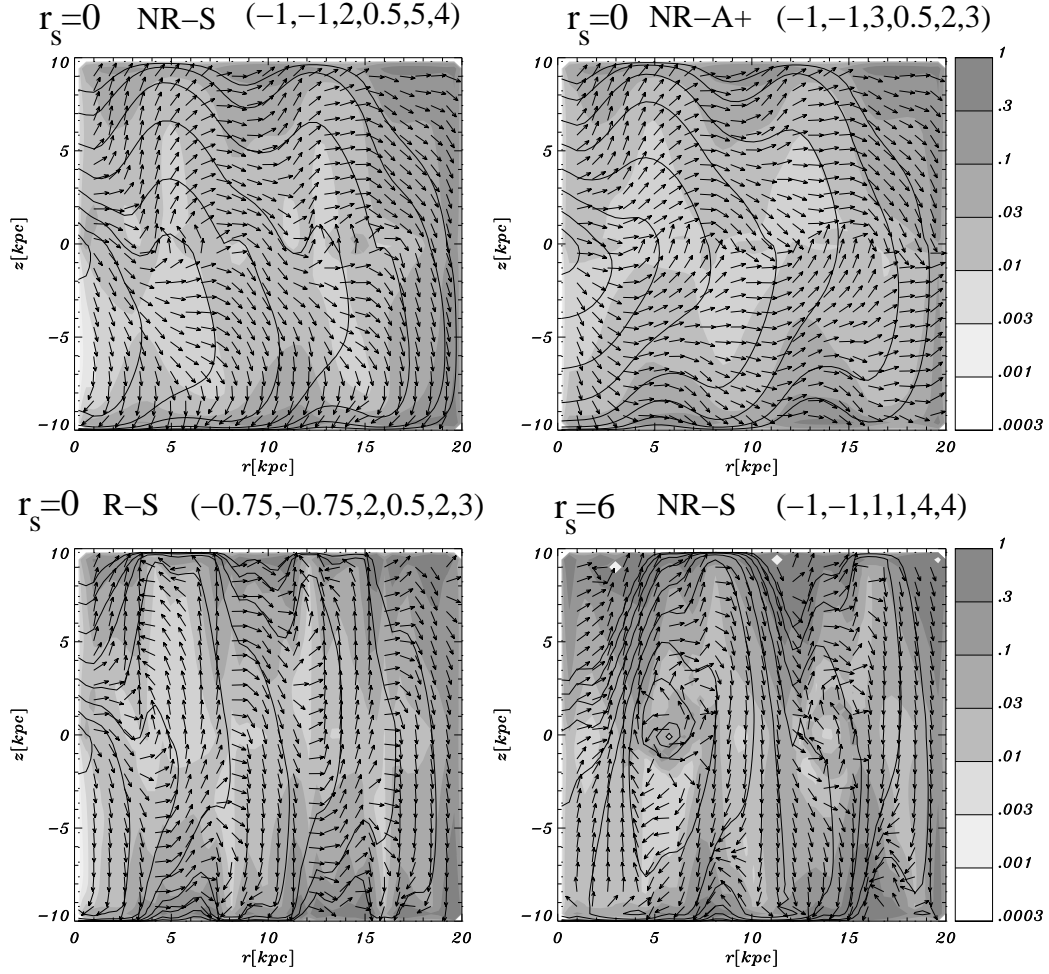


Figure 4: CR densities and drifts for different magnetic field models and source locations. In parenthesis are indicated the values of  $(B_0^{disk}, B_0^{halo}, B_0^{rand}, z_d, z_h, z_r)$  in  $\mu\text{G}$  and kpc respectively.

anticenter deficit observed by AGASA may be reproduced by an overall diffusion flow of the CRs near our location in the direction of the galactic anticenter, with an amplitude leading to a 4% anisotropy [14]. Since one should have reached at the relevant energies the regime in which the drift becomes dominant with respect to the transverse diffusion, and using the fact that locally  $\text{sign}(B_{reg}^\phi) = -1$ , one should have as an approximate estimation that

$$\delta_r \simeq -\frac{3 D_A}{c N} \frac{\partial N}{\partial z} \quad , \quad \delta_z \simeq \frac{3 D_A}{c N} \frac{\partial N}{\partial r}. \quad (5)$$

The overall local asymmetry will then point approximately in the radial direction if locally  $|\partial N/\partial z| \gg |\partial N/\partial r|$ . Its amplitude can be estimated from the expression of the antisymmetric diffusion coefficient, which is

$$D_A \simeq \frac{c r_L}{3} \frac{(\omega \tau_A)^2}{1 + (\omega \tau_A)^2}, \quad (6)$$

where  $r_L$  is the CR Larmor radius (with  $\omega \simeq c/r_L$  the corresponding gyrofrequency) and  $\tau_A$  the relevant time scale of velocity decorrelations (see ref. [9] and references therein). This leads to

$$|\delta_r| \simeq \frac{r_L}{h} \frac{(\omega \tau_A)^2}{1 + (\omega \tau_A)^2} \simeq 0.04 \frac{E}{10^{18} \text{eV}} \frac{26 \text{ kpc}}{Z} \frac{\mu \text{G}}{h} \frac{(\omega \tau_A)^2}{|\mathbf{B}_{reg}| 1 + (\omega \tau_A)^2}, \quad (7)$$

where  $h \equiv |\partial \ln N/\partial z|^{-1}$  is the local vertical scale height of variation of the CR density. Let us notice that due to the mix of different nuclear species present, one has that actually  $\delta = \sum_i f_i \delta_i$ , with  $f_i$  being the fractional abundances of galactic species of charge  $Z_i$  (plotted in figure 2), while  $\delta_i$  their corresponding local anisotropy at the energy under consideration. Although the presence of an extragalactic proton component tends to reduce the fractions  $f_i$ , the nuclei lighter than Fe tend to have larger values of  $\delta_i$  (for some fixed energy), having then the tendency of increasing the value of  $\delta$ . As a result, the values displayed in figures 3.c and 4, which are the anisotropies of Fe nuclei for  $1.5 \times 10^{18}$  eV, are indeed good estimators of the total anisotropy  $\delta$  at this energy.

We see from Eq. (7) that the anisotropies steadily grow with energy, reaching a few % at  $10^{18}$ eV if the typical scale height of the CR density variations are of order a kpc. Significant vertical gradients in the CR density on the galactic plane naturally result in symmetric magnetic field models, since the vertical drifts in those models are similarly oriented in both hemispheres. To have the asymmetry vector pointing away from the galactic center clearly requires the local value of  $\partial N/\partial z$  to be negative, something which generally results when CRs have the tendency to drift to negative values of  $z$ , and this happens more pronouncedly e.g. in models where a symmetric halo field is pointed in the  $-\hat{\phi}$  direction. Also, in order that locally



$|\partial N/\partial r| < |\partial N/\partial z|$  it is convenient that the source be not too close to our location. The model  $NR - A+$  (top right) also shows the interesting feature that drifts tend to converge towards the galactic plane (the opposite would occur in  $A-$  models), resulting in an outward drift for  $z \simeq 0$ . On the contrary, a halo model following the reversals of the disk (or a disk model alone without a regular halo), has very pronounced vertical drifts (bottom left panel). The factor  $(\omega\tau_A)^2/(1 + (\omega\tau_A)^2)$  in Eqs. (6) and (7) reflects the suppression in  $D_A$  in the presence of strong turbulence. It approaches unity if  $B^{rand} < B^{reg}$  but it can become small if the turbulence is large, and this would then suppress the anisotropies.

Let us mention here that other attempts have been made to explain the galactic center excess as resulting from CRs arriving almost rectilinearly from a central source [15, 16, 17]. Even if the CR were protons, the deflection produced by the regular (and random) galactic magnetic fields will largely exceed the  $10^\circ$  displacement between the observed excess and the galactic center direction (to produce this small deflection the source should be closer than  $\sim 2$  kpc [16]). Hence, the hypothesis that the excess is due to neutrons produced from accelerated protons or nuclei through photopion production or spallation processes around the sources in the center of the galaxy has been explored as an alternative explanation [6, 16]. The interesting fact about this proposal is that the decay length of neutrons is just  $\sim 10$  kpc ( $E/10^{18}$  eV), being of the order of the galactocentric distance for the energies relevant for the anisotropies, and hence this would also explain why no significant excess is seen at lower energies. Anyhow, to have such a powerful neutron source is not particularly natural<sup>1</sup>, and furthermore there is no way in which such scenarios can also account for the deficit observed in the anticenter direction.

As regards the excess of events observed from the Cygnus direction, let us notice that a similar explanation to that discussed here can in principle be searched in terms of an overall CR diffusion along the spiral arm. This would clearly require a departure from the assumption of cylindrical symmetry and to take into account the parallel diffusion of CRs along the arms. A general prediction of this kind of scenario would be that a deficit associated to the opposite direction would result, something of potential interest for future observations in the southern hemisphere with the AUGER observatory.

## Acknowledgments

Work supported by CONICET and Fundación Antorchas, Argentina.

---

<sup>1</sup>On the contrary, the maximum energy of galactic protons in our scenario needs not be larger than  $\sim 10^{17}$  eV, a value which is clearly much more plausible.

## References

- [1] Nagano M. and Watson A. A. (2000), *Rev. of Mod. Phys.* **72**, 689.
- [2] Yoshida S. and Dai H. (1998), *J. of Phys. G* **24**, 905.
- [3] Afanasiev B. N., et al. (1993), in *Proc. of the Tokyo Workshop on Techniques for the study of EHECR*, Ed. M. Nagano, p. 35.
- [4] Bird D. J., et al. (1993), *Phys. Rev. Lett.* **71**, 3401.
- [5] Bird D. J., et al. (1994), *Astrophys. J.* **424**, 491.
- [6] Hayashida N., et al. (1999), *Astropart. Phys.* **10**, 303.
- [7] Bellido J. A., et al. (2001), *Astropart. Phys.* **15**, 167.
- [8] Ptuskin V. S. et al. (1993), *Astron. Astrophys.* **268**, 726.
- [9] Candia J., Roulet E. and Epele L. N. (2002), astro-ph/0206336.
- [10] Clay R. W. and Smith G. K. (1996), *Pub. Astron. Soc. Aust.* **13**, 121.
- [11] Ave M., et al. (2002), astro-ph/0203150.
- [12] Abu-Zayyad T. et al. (2001), *Astrophys. J.* **557**, 686.
- [13] Berezhinskii, V. S. et al. (1990), *Astrophysics of Cosmic Rays*, Amsterdam: North Holland.
- [14] Teshima M., et al. (2001), *Proc. of ICRC 2001*, 337.
- [15] Clay R. W. (2000) *Pub. Astron. Soc. Aust.* **17**, 3.
- [16] Medina-Tanco G. A. and Watson A. A. (2001), *Proc. of ICRC 2001*, 531.
- [17] Bednarek W., Giller M. and Zielińska M. (2002), astro-ph/0205324.